

A DYNAMIC SECOND-ORDER ESTIMATION STRATEGY FOR FAULTY SYSTEMS

Hamed H. Afshari,* Andrew S. Lee,** S. Andrew Gadsden,* and Saeid R. Habibi*

Abstract

This paper introduces a novel second-order state estimation method that is applied to linear systems dealing with modelling uncertainties. This method produces state estimates by decreasing the innovation sequence (measurement error) and its time difference which results in preserving smoothness and stability against modelling uncertainties. This filter is referred to as the second-order filter since it updates state estimates based on values of the measurement error and its incremental change. The corrective gain of this filter is designed based on a time-varying manifold that is a linear combination of the measurement error and its time difference. This manifold introduces a cut-off frequency coefficient into the filter formulation. The optimal version of the dynamic second-order filter is then calculated by finding the optimal value of this coefficient at each time step such that the state error covariance matrix is minimised. It is shown that the corrective gain of the optimal second-order filter collapses to the Kalman filter's gain for a known model with white noise. In order to verify the accuracy of the method, it is implemented on an aerospace electro-hydrostatic actuator setup under the normal and faulty scenarios.

Key Words

Estimation theory, faulty systems, Kalman filter, signal processing, sliding modes

1. Introduction

Estimation is the process of extracting the value of a quantity or state from indirect, inaccurate, and uncertain measurements. The main goals are to minimise the estimation error as well as achieving robustness against modelling uncertainties, measurement noise, and bounded disturbances. Noise and disturbances are inherently present in the measurement process and are caused by instruments

and environmental factors. Other uncertainties are caused by perturbations or inherent inaccuracy in modelling, including variations of physical parameters due to system deteriorations or ageing. Parameter and state estimation are increasingly used in real-time control and monitoring applications.

Optimality in estimation has usually been obtained by adjusting a filter's corrective gain to minimise the state error covariance. The Wiener–Kolmogorov filter was one of the first major contributions in optimal estimation that was proposed for stationary signals. It assumed estimates with known spectral properties subject to white noise. The Kalman filter was a generalisation of the Wiener–Kolmogorov filter and has been applied to linear systems with non-stationary Gaussian signals [1]. The Kalman filter is optimal for a linear system with a perfectly known model subject to white process noise and measurement noise. Under these assumptions, the Kalman filter recursively computes the optimal states using a predictor–corrector algorithm using an optimal gain. The Kalman filter gain is calculated such that the state error covariance matrix is minimised as each time sample.

Another important consideration in estimation is robustness to modelling uncertainties and bounded disturbances. Considerable research has been performed on the design of robust state estimation methods for dynamic systems with bounded uncertainties, such as minimax estimators, worst-case, or set-membership state estimators [2]–[4]. From the statistical standpoint, the minimax estimators deal with uncertainties that are uniformly distributed within a given bound. In the case of ellipsoidal bounding sets, these estimators coincide with the Kalman filter for linear systems. Other strategies found in literature include the robust Kalman filter [5]–[8], the H_∞ filter [9]–[11], and variable structure filtering (VSF) [12]–[14]. Xie *et al.* [5] have presented a robust Kalman filter method that is robust versus time-varying norm-bounded parametric uncertainties in the state and measurement matrices. Their filter applies to linear systems with modelling uncertainty and guarantees that the variance of measurement error remains norm-bounded [5]. The robust Kalman filter was moreover designed for systems with bounded modelling uncertainties such that an upper bound of the mean square estimation error is minimised at each step [7]. Zames [15] proposed the H_∞ method in 1980 that removed the necessity of a perfect model or complete knowledge of

* Department of Mechanical Engineering, McMaster University, Hamilton, Ontario, Canada, L8S 4L8; e-mail: h.h.afshari@gmail.com; {gadsden,habibi}@mcmaster.ca

** College of Engineering and Physical Sciences, University of Guelph, 50 Stone Road East, Guelph, Ontario, Canada, N1G 2W1; e-mail: andy.lee.guelph@gmail.com
Corresponding Author: S. Andrew Gadsden

the input statistics. The H_∞ theory was designed based on tracking the energy of a signal for the worst possible values of noise and modelling uncertainties [16].

The smooth variable structure filter (SVSF) is a model-based robust state estimation strategy [12]. It is based on the concept of variable structure systems that achieves stability given an upper bound for modelling uncertainties and noise levels [12]. Gadsden developed the optimal version of the SVSF filter and presented applications for fault diagnosis [14], [17]. Mahalanabis *et al.* [18] presented a second-order method for state estimation of nonlinear systems. Their method was restricted to a class of nonlinear systems subjected to a Gaussian noise distribution. They showed that a nonlinear state equation may be expanded using a polynomial function of arbitrary order and developed a second-order state estimation method based on the nonlinear state model with first-order differential equations [18]. Afshari modeled the dynamics of actuation systems using physical methods [19], [20] and designed filters for robust state estimation for actuation systems under normal and faulty cases [21]–[23].

This paper presents a dynamic second-order filter that is applied to systems with linear state and measurement models. Its corrective gain is formulated as a second-order Markov process and is designed based on a manifold that is a linear combination of the innovation sequence (measurement error) and its time difference. The stability of the dynamic second-order filter under the manifold is proven using the Lyapunov's second law of stability. The stability criterion results in convergence and an iterative decrease in the measurement error and its time difference. In addition to its initial formulation, an optimal version of the dynamic second-order filter is then presented that minimises the state error covariance. It is shown that the corrective gain of the optimal second-order filter collapses to the Kalman filter's gain given white noise. An experimental electro-hydrostatic actuator (EHA) setup is used to show the improved performance of the dynamic second-order filter over the robust Kalman filter and the SVSF method.

2. The Dynamic Second-Order Filter for State Estimation

Consider a dynamic system defined by linear state and measurement models in discrete time as follows:

$$\mathbf{x}_{k+1} = \mathbf{F}\mathbf{x}_k + \mathbf{G}\mathbf{u}_k + \mathbf{w}_k \quad (1)$$

$$\mathbf{z}_{k+1} = \mathbf{H}\mathbf{x}_{k+1} + \mathbf{v}_{k+1} \quad (2)$$

where $\mathbf{x} \in \mathbb{R}^{n \times 1}$ is the state vector, $\mathbf{u} \in \mathbb{R}^{p \times 1}$ is the control vector, and $\mathbf{z} \in \mathbb{R}^{m \times 1}$ is the measurement vector. $\mathbf{F} \in \mathbb{R}^{n \times n}$ is the state matrix, $\mathbf{G} \in \mathbb{R}^{n \times p}$ is the control matrix, $\mathbf{H} \in \mathbb{R}^{m \times n}$ is the measurement matrix, and $\mathbf{w} \in \mathbb{R}^{n \times 1}$ and $\mathbf{v} \in \mathbb{R}^{m \times 1}$ are the process noise and the measurement noise, respectively. The following assumptions are made in the derivation of the dynamic second-order filter.

Assumption 1. *Vectors \mathbf{w} and \mathbf{v} are mutually independent random variables and have a truncated Gaussian distribution with a zero mean. Their amplitudes are,*

respectively, bounded by w_{\max} and v_{\max} such that:

$$\begin{cases} |w_{i, k}| \leq w_{\max}; i = 1, \dots, n \\ |v_{i, k}| \leq v_{\max}; i = 1, \dots, m \end{cases} \quad (3)$$

It is moreover assumed that they are statistically independent with respect to the state vector $\mathbf{x} \in \mathbb{R}^{n \times 1}$.

Assumption 2. *It is assumed that the system with (1) and (2) is completely observable. The measurement matrix \mathbf{H} is assumed to be invertible. For cases where $m \neq n$, the pseudo-inverse of the \mathbf{H} matrix, namely, \mathbf{H}^+ , is calculated using the Moore–Penrose pseudo-inverse.*

Definition 1. *Let Δ be the backward difference operator that applies to variable x such that: $\Delta\mathbf{x}_{k+1} = \mathbf{x}_{k+1} - \mathbf{x}_k$. It is assumed that Δ is a smooth differentiable operator.*

The dynamic second-order filter applies to systems with linear state and measurement models in a predictor–corrector form. It is summarised in the following prediction and update steps.

1. Prediction step:

- Prediction of the *a priori* state estimate $\hat{\mathbf{x}}_{k+1|k}$ using the previous *a posteriori* state estimate $\hat{\mathbf{x}}_{k|k}$, is calculated as follows:

$$\hat{\mathbf{x}}_{k+1|k} = \hat{\mathbf{F}}\hat{\mathbf{x}}_{k|k} + \hat{\mathbf{G}}\mathbf{u}_k \quad (4)$$

Prediction of the *a priori* measurement $\hat{\mathbf{z}}_{k+1|k}$, is calculated as follows:

$$\hat{\mathbf{z}}_{k+1|k} = \hat{\mathbf{H}}\hat{\mathbf{x}}_{k+1|k} \quad (5)$$

Note that $\hat{\mathbf{F}}$, $\hat{\mathbf{G}}$, and $\hat{\mathbf{H}}$ are, respectively, the estimated state matrix, control matrix, and measurement matrix. It is assumed that $\hat{\mathbf{H}} \simeq \mathbf{H}$, $\hat{\mathbf{F}} \simeq \mathbf{F}$, and $\hat{\mathbf{G}} \simeq \mathbf{G}$.

- Calculation of the *a priori* and the *a posteriori* measurement error vectors, $\mathbf{e}_{\mathbf{z}_{k+1|k}} \in \mathbb{R}^{m \times 1}$ and $\mathbf{e}_{\mathbf{z}_{k|k}} \in \mathbb{R}^{m \times 1}$ as:

$$\mathbf{e}_{\mathbf{z}_{k+1|k}} = \mathbf{z}_{k+1} - \hat{\mathbf{H}}\hat{\mathbf{x}}_{k+1|k} \quad (6)$$

$$\mathbf{e}_{\mathbf{z}_{k|k}} = \mathbf{z}_k - \hat{\mathbf{H}}\hat{\mathbf{x}}_{k|k} \quad (7)$$

2. Update step:

- The corrective gain $\mathbf{K} \in \mathbb{R}^{n \times m}$ is obtained as a function of the *a priori* $\mathbf{e}_{\mathbf{z}_{k+1|k}}$, the *a posteriori* $\mathbf{e}_{\mathbf{z}_{k|k}}$, the $\mathbf{e}_{\mathbf{z}_{k-1|k-1}}$ measurement errors, and the cut-off frequency matrix as follows:

$$\mathbf{K}_{k+1} = \mathbf{f}(\hat{\mathbf{H}}, \mathbf{\Lambda}, \mathbf{e}_{\mathbf{z}_{k+1|k}}, \mathbf{e}_{\mathbf{z}_{k|k}}, \mathbf{e}_{\mathbf{z}_{k-1|k-1}}) \quad (8)$$

where $\mathbf{\Lambda} \in \mathbb{R}^{m \times m}$ is the cut-off frequency matrix and represents the filter's bandwidth. Note that in order to calculate the corrective gain function \mathbf{f} , the measurement matrix \mathbf{H} and its estimate $\hat{\mathbf{H}}$ are non-singular. They are initially assumed to be square

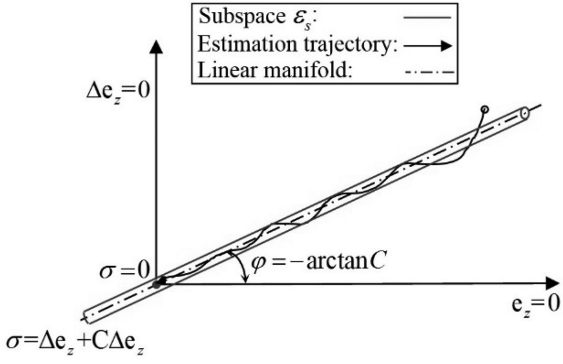


Figure 1. Dynamic second-order filter based on a linear manifold.

matrices indicating that all states are measured $m = n$. Section 5 presents the gain \mathbf{K} for systems without full state measurement $m \neq n$.

- The *a priori* state estimate is updated into the *a posteriori* state estimate as follows:

$$\hat{\mathbf{x}}_{k+1|k+1} = \hat{\mathbf{x}}_{k+1|k} + \mathbf{K}_{k+1} \mathbf{e}_{z_{k+1|k}} \quad (9)$$

The proof of stability for the dynamic second-order filter is obtained by defining a manifold that is a linear combination of the measurement error and its time difference as follows:

$$\boldsymbol{\sigma}_k = \Delta \mathbf{e}_{z_{k|k}} + \mathbf{C} \mathbf{e}_{z_{k|k}} \quad (10)$$

where $\boldsymbol{\sigma}_k : \mathbb{R}^{m \times 1} \rightarrow \mathbb{R}^{m \times 1}$ is the linear manifold, $\mathbf{e}_{z_{k|k}} \in \mathbb{R}^{m \times 1}$ is the measurement error (innovation sequence), $\mathbf{C} = \mathbf{Diag}() \in \mathbb{R}^{m \times m}$ is a diagonal matrix with entries c_{ii} . In a geometrical sense, matrix \mathbf{C} is related to the slope of the manifold in a phase plane, with coordinates $\Delta \mathbf{e}_{z_{k|k}}$ and $\mathbf{e}_{z_{k|k}}$. Figure 1 presents the concept of the dynamic second-order filter in a phase plane.

Remark 1. The linear manifold $\boldsymbol{\sigma}_k = \Delta \mathbf{e}_{z_{k|k}} + \mathbf{C} \mathbf{e}_{z_{k|k}}$ presents a first-order low-pass filter, where \mathbf{C} is referred to as the manifold cut-off frequency matrix. Taking the Z-transform of the manifold, the measurement error $e_{i,z}$ is given by:

$$e_{i,z}(z) = \frac{1}{1 + c_{ii} - z^{-1}} \sigma_i(z) \quad (11)$$

Rearranging (11) gives $e_{i,z}(z) = \frac{z}{(1+c_{ii})z-1} \sigma_i(z)$. Hence, the measurement error $e_{i,z}(z)$ may be synthesised as the output of a first-order low-pass filter with a bandwidth that is a function of the manifold slope c_{ii} . By proper selection of elements c_{ii} , it is possible to apply an internal filtering strategy with variable bandwidths for removing unwanted high-frequency dynamics. Furthermore, the entry c_{ii} denotes the cut-off frequency corresponding to the i^{th} element of the measurement error $e_{i,z} \in \mathbf{e}_z$. Its value adjusts the filter's bandwidth which affects the smoothness of state estimates. Using an internal filtering method with its own cut-off frequency, the coefficient is one of the main

advantages of the dynamic second-order filter over other state estimation methods.

3. Corrective Gain for the Dynamic Second-Order Filter

A corrective gain $\mathbf{K} \in \mathbb{R}^{n \times m}$ for the dynamic second-order filter given a full measurement matrix $\widehat{\mathbf{H}} \in \mathbb{R}^{n \times m}$ ($m = n$) is as follows:

$$\mathbf{K}_{k+1} = \widehat{\mathbf{H}}^{-1} \left[\mathbf{e}_{z_{k+1|k}} - (\boldsymbol{\gamma} + \boldsymbol{\Lambda}) \mathbf{e}_{z_{k|k}} + \boldsymbol{\gamma} \boldsymbol{\Lambda} \mathbf{e}_{z_{k-1|k-1}} \right] \left[\mathbf{e}_{z_{k+1|k}} \right]^+ \quad (12)$$

where $\boldsymbol{\Lambda} \in \mathbb{R}^{m \times m}$ is the cut-off frequency matrix, and $\boldsymbol{\gamma} = \mathbf{Diag}(\gamma_{ii}) \in \mathbb{R}^{m \times m}$ is a diagonal matrix with positive entries such that $0 < \gamma_{ii} < 1$ represents the convergence rate. $[\mathbf{e}_{z_{k+1|k}}]^+$ is the pseudo-inverse of the *a priori* measurement error vector and is calculated using the Moore–Penrose pseudo-inverse.

Theorem 1. Assume a linear discrete system with the state and measurement models of (1) and (2). The dynamic second-order filter with the corrective gain (12) is stable and produces convergent state estimates.

Proof. Consider a positive-definite Lyapunov function as:

$$V_k = \sigma_{i,k}^2 \quad (13)$$

where $\sigma_i \in \mathbb{R}$ is an element of the linear manifold and defined as: $\sigma_{i,z_{k|k}} = \Delta e_{i,z_{k|k}} + c_{ii} e_{i,z_{k|k}}$. Furthermore, $\Delta e_{i,z} \in \mathbb{R}$ denotes the difference of the measurement error $e_{i,z_{k|k}}$ and is calculated as $\Delta e_{i,z_{k|k}} = e_{i,z_{k|k}} - e_{i,z_{k-1|k-1}}$. The dynamic second-order filter is stable if $\Delta V_{k+1} = V_{k+1} - V_k < 0$. Substituting the Lyapunov function in this inequality yields: $\Delta V_{k+1} = (\Delta e_{i,z_{k+1|k+1}} + e_{i,z_{k+1|k+1}})^2 - (\Delta e_{i,z_{k|k}} + e_{i,z_{k|k}})^2$, where $\Delta e_{i,z_{k+1|k+1}} = e_{i,z_{k+1|k+1}} - e_{i,z_{k|k}}$ and $\Delta e_{i,z_{k|k}} = e_{i,z_{k|k}} - e_{i,z_{k-1|k-1}}$. By substituting these values and rearranging, ΔV_{k+1} is obtained as:

$$\Delta V_{k+1} = (1 + c_{ii})^2 e_{i,z_{k+1|k+1}}^2 - 2(1 + c_{ii}) e_{i,z_{k+1|k+1}} e_{i,z_{k|k}} - 2c_{ii} (1 + c_{ii}) e_{i,z_{k|k}} e_{i,z_{k-1|k-1}} - e_{i,z_{k-1|k-1}}^2 \quad (14)$$

For simplicity, let elements of the manifold's cut-off frequency matrix be defined as:

$$\lambda_{ii} = \frac{1}{1 + c_{ii}} \quad (15)$$

where $\boldsymbol{\Lambda} = \mathbf{Diag}(\lambda_{ii}) \in \mathbb{R}^{m \times m}$ is a diagonal matrix. This definition simplifies the calculation of the derivative of the error covariance with respect to the manifold cut-off frequency.

Multiplying the gain equation (12) by $\widehat{\mathbf{H}}$, and then by $\mathbf{e}_{z_{k+1|k}}$, and rearranging gives:

$$\mathbf{e}_{z_{k+1|k}} - \widehat{\mathbf{H}} \mathbf{K}_{k+1} \mathbf{e}_{z_{k+1|k}} = (\boldsymbol{\gamma} + \boldsymbol{\Lambda}) \mathbf{e}_{z_{k|k}} - \boldsymbol{\gamma} \boldsymbol{\Lambda} \mathbf{e}_{z_{k-1|k-1}} \quad (16)$$

As the estimated states are updated using (9), $\hat{\mathbf{x}}_{k+1|k+1} = \hat{\mathbf{x}}_{k+1|k} + \mathbf{K}_{k+1} \mathbf{e}_{z_{k+1|k}}$, it leads to:

$\mathbf{K}_{k+1}\mathbf{e}_{z_{k+1}|k} = \widehat{\mathbf{x}}_{k+1|k+1} - \widehat{\mathbf{x}}_{k+1|k}$. Substituting this relation into (16) leads to:

$$\mathbf{e}_{z_{k+1}|k} - \widehat{\mathbf{H}}(\widehat{\mathbf{x}}_{k+1|k+1} - \widehat{\mathbf{x}}_{k+1|k}) = (\gamma + \mathbf{\Lambda})\mathbf{e}_{z_k|k} - \gamma\mathbf{\Lambda}\mathbf{e}_{z_{k-1}|k-1} \quad (17)$$

The *a priori* and the *a posteriori* measurement errors at time step k are obtained from (6) and (7) as: $e_{z_{k+1}|k} = z_{k+1} - \widehat{\mathbf{H}}\widehat{\mathbf{x}}_{k+1|k}$, and $e_{z_{k+1}|k+1} = z_{k+1} - \widehat{\mathbf{H}}\widehat{\mathbf{x}}_{k+1|k+1}$. Subtracting the *a priori* error from the *a posteriori* error leads to:

$$\mathbf{e}_{z_{k+1}|k+1} - \mathbf{e}_{z_{k+1}|k} = -\widehat{\mathbf{H}}(\widehat{\mathbf{x}}_{k+1|k+1} - \widehat{\mathbf{x}}_{k+1|k}) \quad (18)$$

From (19), it is possible to restate equality (17) as:

$$\mathbf{e}_{z_{k+1}|k+1} = (\gamma + \mathbf{\Lambda})\mathbf{e}_{z_k|k} - \gamma\mathbf{\Lambda}\mathbf{e}_{z_{k-1}|k-1} \quad (19)$$

Equality (19) can be restated in terms of its entries $e_{i,z}$, where γ and Δ are diagonal matrices, as:

$$e_{i,z_{k+1}|k+1} = (\gamma_{ii} + \lambda_{ii})e_{i,z_k|k} - \gamma_{ii}\lambda_{ii}e_{i,z_{k-1}|k-1} \quad (20)$$

In order to show the negative definiteness of the Lyapunov function candidate defined by (13), equality (20) is substituted into (14). Expanding the result:

$$\Delta V_{k+1} = (\gamma_{ii}^2 - 1)(1 + \lambda_{ii})^2 e_{i,z_k|k}^2 + (\gamma_{ii}^2 - 1)e_{i,z_{k-1}|k-1}^2 - 2(\gamma_{ii}^2 - 1)(1 + \lambda_{ii})e_{i,z_k|k}e_{i,z_{k-1}|k-1} \quad (21)$$

Rearranging equality (21) results in:

$$\Delta V_{k+1} = (\gamma_{ii}^2 - 1)[(1 + \lambda_{ii})e_{i,z_k|k} - e_{i,z_{k-1}|k-1}]^2 \quad (22)$$

As the convergence rate matrix $\gamma = \mathbf{Diag}(\gamma_{ii}) \in \mathbb{R}^{m \times m}$ is defined such that $0 < \gamma_{ii} < 1$, it leads to $\Delta V_{k+1} < 0$ which proves the stability of the dynamic second-order filter under gain (12). \square

Remark 2. If the Lyapunov function (13) is satisfied, then $|\sigma_{k+1}| < |\sigma_k|$. As $\sigma_k = \Delta e_{z_k|k} + \mathbf{C}e_{z_k|k}$, it shows that the summation of the measurement error and its time difference is decreasing over time.

Remark 3. The corrective gain (12) actually represents a second-order Markov process that is formulated in terms of the measurement error at time steps k and $k - 1$. Using a second-order corrective gain in the update step results in updating the state estimates based on information available from the last two steps. Having access to higher amount of information from the past intuitively increases smoothness of state estimates in comparison to estimates generated from a first-order filter.

Lemma 1. The state estimation error $\mathbf{e}_{\mathbf{x}_k|k} = \mathbf{x}_k - \widehat{\mathbf{x}}_k|k$ generated from the dynamic second-order filter remains norm-bounded given norm-bounded process and measurement noise.

Proof. The state estimation error $\mathbf{e}_{\mathbf{x}_{k+1}|k+1}$ is calculated by:

$$\mathbf{e}_{\mathbf{x}_{k+1}|k+1} = \mathbf{x}_{k+1} - \widehat{\mathbf{x}}_{k+1|k+1} \quad (23)$$

where $\widehat{\mathbf{x}}_{k+1|k+1} = \widehat{\mathbf{x}}_{k+1|k} + \mathbf{K}_{k+1}\mathbf{e}_{z_{k+1}|k}$. Moreover, \mathbf{x}_{k+1} and $\widehat{\mathbf{x}}_{k+1|k}$ are obtained from (1) and (4), respectively. Hence, $\mathbf{e}_{\mathbf{x}_{k+1}|k+1}$ is given by:

$$\mathbf{e}_{\mathbf{x}_{k+1}|k+1} = \mathbf{x}_{k+1} - \widehat{\mathbf{x}}_{k+1|k+1} = \mathbf{F}\mathbf{x}_k|k + \mathbf{G}\mathbf{u}_k + \mathbf{w}_k - \left(\widehat{\mathbf{F}}\widehat{\mathbf{x}}_k|k + \widehat{\mathbf{G}}\mathbf{u}_k + \mathbf{K}_{k+1}\mathbf{e}_{z_{k+1}|k} \right) \quad (24)$$

where the gain \mathbf{K} is given by (12). Assuming $\widehat{\mathbf{H}} = \mathbf{H}$, $\widehat{\mathbf{F}} = \mathbf{F}$, and $\widehat{\mathbf{G}} = \mathbf{G}$, equality (24) may be simplified as:

$$\mathbf{e}_{\mathbf{x}_{k+1}|k+1} = \widehat{\mathbf{F}}(\mathbf{x}_k - \widehat{\mathbf{x}}_k|k) + \mathbf{w}_k - \mathbf{K}_{k+1}\mathbf{e}_{z_{k+1}|k} \quad (25)$$

which is equal to $\mathbf{e}_{\mathbf{x}_{k+1}|k+1} = \widehat{\mathbf{F}}\mathbf{e}_{\mathbf{x}_k|k} + \mathbf{w}_k - \mathbf{K}_{k+1}\mathbf{e}_{z_{k+1}|k}$. By substituting \mathbf{K} from equality (12) into the above equality and simplifying the resulting terms, it becomes:

$$\mathbf{e}_{\mathbf{x}_{k+1}|k+1} = \widehat{\mathbf{F}}\mathbf{e}_{\mathbf{x}_k|k} + \mathbf{w}_k - \left[\mathbf{e}_{z_{k+1}|k} - (\gamma + \mathbf{\Lambda})\mathbf{e}_{z_k|k} + \gamma\mathbf{\Lambda}\mathbf{e}_{z_{k-1}|k-1} \right] \quad (26)$$

As $z_{k+1} = \mathbf{H}\mathbf{x}_{k+1} + \mathbf{v}_{k+1}$, and $\widehat{z}_{k+1|k} = \widehat{\mathbf{H}}\widehat{\mathbf{x}}_{k+1|k}$, measurement errors $\mathbf{e}_{z_{k+1}|k+1}$, $\mathbf{e}_{z_{k+1}|k}$, and $\mathbf{e}_{z_k|k}$ may be restated in terms of $\mathbf{e}_{\mathbf{x}_k|k}$ and $\mathbf{e}_{\mathbf{x}_{k+1}|k+1}$, as follows:

$$\begin{aligned} \mathbf{e}_{z_{k+1}|k+1} &= \widehat{\mathbf{H}}\mathbf{e}_{\mathbf{x}_{k+1}|k+1} + \mathbf{v}_{k+1} \\ \mathbf{e}_{z_{k+1}|k} &= \widehat{\mathbf{H}}\widehat{\mathbf{F}}\mathbf{e}_{\mathbf{x}_k|k} + \widehat{\mathbf{H}}\mathbf{w}_k + \mathbf{v}_{k+1} \\ \mathbf{e}_{z_k|k} &= \widehat{\mathbf{H}}\mathbf{e}_{\mathbf{x}_k|k} + \mathbf{v}_k \end{aligned} \quad (27)$$

Substituting the above equalities into (26) and simplifying it, $\mathbf{e}_{\mathbf{x}_{k+1}|k+1}$ is obtained as follows:

$$\mathbf{e}_{\mathbf{x}_{k+1}|k+1} = (\gamma + \mathbf{\Lambda})\mathbf{e}_{\mathbf{x}_k|k} - \gamma\mathbf{\Lambda}\mathbf{e}_{\mathbf{x}_{k-1}|k-1} - \widehat{\mathbf{H}}^{-1}\mathbf{v}_{k+1} + (\gamma + \mathbf{\Lambda})\widehat{\mathbf{H}}^{-1}\mathbf{v}_k - \gamma\Delta\widehat{\mathbf{H}}^{-1}\mathbf{v}_{k-1} \quad (28)$$

Following *Assumption 1*, \mathbf{v} is a zero-mean noise with a truncated Gaussian distribution. Therefore, by taking the expectation of equality (28), the terms that contain the measurement noise \mathbf{v} are cancelled and the state estimation error equation is obtained as follows:

$$\bar{\mathbf{e}}_{\mathbf{x}_{k+1}|k+1} - (\gamma + \mathbf{\Lambda})\bar{\mathbf{e}}_{\mathbf{x}_k|k} + \gamma\mathbf{\Lambda}\bar{\mathbf{e}}_{\mathbf{x}_{k-1}|k-1} = 0 \quad (29)$$

where $\bar{\mathbf{e}}_{\mathbf{x}_k|k}$ is the expectation of $\mathbf{e}_{\mathbf{x}_k|k}$. Taking the z-transform of equality (29), it becomes:

$$\left[z^2 - (\gamma + \mathbf{\Lambda})z + \gamma\mathbf{\Lambda} \right] \bar{\mathbf{e}}_{\mathbf{x}}(z) = 0 \quad (30)$$

A necessary and sufficient condition for stability of the state estimation error (its expectation) is that γ and Δ are tuned such that the poles of (30) are within the unit circle. \square

4. The Optimal Second-Order Filter for State Estimation

In order to optimise the dynamic second-order filter in terms of the mean-squared error, it is necessary to introduce the state error covariance matrix into the filter formulation. The error covariance matrix provides additional information about the state estimate's dispersion for the filter that in turns results in more

accurate estimates. The calculation process of the *a priori* and *a posteriori* state error covariance for the new derivation is similar to what was presented by Gadsden and Habibi [12], [14], [20] for the SVSF method based on the Kalman filter [1], [14]. The *a priori* state error covariance matrix is defined as follows [14]:

$$\mathbf{P}_{k+1|k} = E \{ (\mathbf{x}_{k+1} - \hat{\mathbf{x}}_{k+1|k})(\mathbf{x}_{k+1} - \hat{\mathbf{x}}_{k+1|k})^T \} \quad (31)$$

As $\mathbf{x}_{k+1} = \mathbf{F}\mathbf{x}_k + \mathbf{G}\mathbf{u}_k + \mathbf{w}_k$, and $\hat{\mathbf{x}}_{k+1} = \hat{\mathbf{F}}\mathbf{x}_k + \hat{\mathbf{G}}\mathbf{u}_k$, it leads to:

$$\begin{aligned} \mathbf{P}_{k+1|k} = E \{ & \hat{\mathbf{F}}\mathbf{e}_{\mathbf{x}_{k+1|k}}\mathbf{e}_{\mathbf{x}_{k+1|k}}^T \hat{\mathbf{F}}^T + \hat{\mathbf{F}}\mathbf{e}_{\mathbf{x}_{k+1|k}}\mathbf{w}_k^T \\ & + \mathbf{w}_k\mathbf{e}_{\mathbf{x}_{k+1|k}}^T \hat{\mathbf{F}}^T + \mathbf{w}_k\mathbf{w}_k^T \} \end{aligned} \quad (32)$$

Further to *Assumption 1*:

$$E \{ \mathbf{w}_k \} = E \{ \mathbf{w}_k^T \} = 0 \quad (33)$$

$$E \{ \mathbf{e}_{\mathbf{x}_{k+1|k}}\mathbf{w}_k^T \} = E \{ \mathbf{w}_k\mathbf{e}_{\mathbf{x}_{k+1|k}}^T \} = 0 \quad (34)$$

$$E \{ \mathbf{w}_k\mathbf{w}_k^T \} = \mathbf{Q}_k \quad (35)$$

where \mathbf{Q} is the process noise covariance. The *a priori* state covariance matrix is given by [14]:

$$\mathbf{P}_{k+1|k} = \hat{\mathbf{F}}\mathbf{P}_{k|k}\hat{\mathbf{F}}^T + \mathbf{Q}_k \quad (36)$$

Similarly, the *a posteriori* error covariance matrix is given by:

$$\begin{aligned} \mathbf{P}_{k+1|k+1} = & (\mathbf{I} - \mathbf{K}_{k+1}\hat{\mathbf{H}})\mathbf{P}_{k+1|k}(\mathbf{I} - \mathbf{K}_{k+1}\hat{\mathbf{H}})^T \\ & + \mathbf{K}_{k+1}\mathbf{R}_{k+1}\mathbf{K}_{k+1}^T \end{aligned} \quad (37)$$

where \mathbf{R} denotes the measurement noise covariance [14].

In order to extract the optimal state estimates using the dynamic second-order filter, the optimal value of the cut-off frequency coefficient must be found at each time step. The proposed strategy for finding the optimal cut-off frequency matrix is to calculate the partial derivative of the trace of the state error covariance matrix \mathbf{P} with respect to the cut-off frequency matrix Δ . It results in determining the optimal value of the cut-off frequency at each time and calculates the filter's bandwidth as a function of modelling uncertainties. In the Kalman filter, the gain is calculated to directly minimise the trace of the error covariance matrix. However, in the dynamic second-order filter, the filter's corrective gain is first derived to be within a range that preserves the Lyapunov's second law, where the cut-off frequency matrix is assumed to be constant. Thereafter, the optimal value of the cut-off frequency matrix (filter's bandwidth) is calculated using optimisation.

In the stability-oriented design of the dynamic second-order filter, the cut-off frequency matrix is set to be diagonal. Each diagonal entry λ_{ii} represents the cut-off frequency related to a measurement error which makes the cut-off frequency coefficients independent of each other. A direct consequence of this is that the measurement error of each state $\mathbf{e}_{z_k|k}$ is directly filtered out with a pre-determined bandwidth. Due to the diagonal consideration of the cut-off frequency matrix, coupling effects were neglected in the derivation of the dynamic second-order

filter. In this context, only diagonal entries of the state error covariance matrix are minimised and the off-diagonal entries are neglected. Limiting the filter to having a diagonal cut-off frequency matrix precludes an optimal solution. As such, for optimising the dynamic second-order filter, the cut-off frequency matrix $\mathbf{\Lambda} \in \mathbb{R}^{m \times m}$ needs to be full with diagonal and off-diagonal entries as follows:

$$\mathbf{\Lambda}_k = \begin{bmatrix} \lambda_{11,k} & \lambda_{12,k} & \cdots & \lambda_{1m,k} \\ \lambda_{21,k} & \lambda_{22,k} & \cdots & \lambda_{2m,k} \\ \vdots & \vdots & \ddots & \vdots \\ \lambda_{m1,k} & \lambda_{m2,k} & \cdots & \lambda_{mm,k} \end{bmatrix} \quad (38)$$

where λ_{ii} is a diagonal entry and denotes the cut-off frequency applied on $e_{i,z}$. Otherwise, λ_{ij} is an off-diagonal entry and corresponds to measurement errors $e_{i,z}$ and $e_{j,z}$. *Theorem 2* is presented to introduce the optimal value of the cut-off frequency matrix at each time step. Thereafter, it is shown that the corrective gain of the optimal second-order filter collapses to the Kalman filter's gain.

Theorem 2. *Assume a linear system described by the state and measurement models of (1) and (2). The state error covariance matrix \mathbf{P} (trace) is minimised for the optimal second-order filter, if the cut-off frequency matrix is given by:*

$$\mathbf{\Lambda}_{k+1} = \begin{bmatrix} \text{Diag} (e_{z_{k+1|k}} - \gamma e_{z_k|k}) S_{k+1} - \hat{\mathbf{H}}\mathbf{P}_{k+1|k}\hat{\mathbf{H}}^T \\ \text{Diag} (e_{z_k|k} - \gamma e_{z_{k-1|k-1}}) S_{k+1} \end{bmatrix}^{-1} \text{Diag} (e_{z_{k+1|k}}) \quad (39)$$

Proof. In order to minimise \mathbf{P} with optimal selection of the cut-off frequency $\mathbf{\Lambda}$, its partial derivative (trace) with respect to $\mathbf{\Lambda}$ is calculated such that:

$$\frac{\partial [\text{trace}(\mathbf{P}_{k+1|k+1})]}{\partial \mathbf{\Lambda}_{k+1}} = 0 \quad (40)$$

The error covariance matrix \mathbf{P} is presented by (37), where it contains the gain \mathbf{K} (12). For calculating the partial derivative of equation (40), some relations from the gradient matrix rules are required, including [24]:

$$\frac{\partial [\text{trace}(\mathbf{A}\mathbf{X}\mathbf{B})]}{\partial \mathbf{X}} = \mathbf{A}^T\mathbf{B}^T \quad (41)$$

$$\frac{\partial [\text{trace}(\mathbf{A}\mathbf{X}^T\mathbf{B})]}{\partial \mathbf{X}} = \mathbf{B}\mathbf{A} \quad (42)$$

$$\frac{\partial [\text{trace}(\mathbf{A}\mathbf{X}\mathbf{B}\mathbf{X}^T\mathbf{C})]}{\partial \mathbf{X}} = \mathbf{A}^T\mathbf{C}^T\mathbf{X}\mathbf{B}^T + \mathbf{C}\mathbf{A}\mathbf{X}\mathbf{B} \quad (43)$$

Some matrices, such as \mathbf{P} , are symmetric which simplifies calculations. Substituting the corrective gain (12) into the state error covariance (37) and expanding the

resulting terms lead to the following four parts:

$$\text{Part 1 : } \mathbf{P}_{k+1|k+1}, \quad (44)$$

$$\begin{aligned} \text{Part 2 : } & -\widehat{\mathbf{H}}^{-1} \left[\text{Diag} (e_{z_{k+1}|k} - \gamma e_{z_k|k}) \right. \\ & \left. - \mathbf{\Lambda}_{k+1} \text{Diag} (e_{z_k|k} - \gamma e_{z_{k-1}|k-1}) \right] \\ & [\text{Diag} (e_{z_{k+1}|k})]^{-1} \widehat{\mathbf{H}} \mathbf{P}_{k+1|k}, () \end{aligned} \quad (45)$$

$$\begin{aligned} \text{Part 3 : } & -\mathbf{P}_{k+1|k} \widehat{\mathbf{H}}^T \left[\text{Diag} (e_{z_{k+1}|k} - \gamma e_{z_k|k})^T \right. \\ & \left. - \text{Diag} (e_{z_k|k} - \gamma e_{z_{k-1}|k-1})^T \mathbf{\Lambda}_{k+1}^T \right] \\ & [\text{Diag} (e_{z_{k+1}|k})]^{-1} \widehat{\mathbf{H}}^{-T} \end{aligned} \quad (46)$$

$$\begin{aligned} \text{Part 4 : } & \widehat{\mathbf{H}}^{-1} \left[\text{Diag} (e_{z_{k+1}|k} - \gamma e_{z_k|k})^T \right. \\ & \left. - \mathbf{\Lambda}_{k+1} \text{Diag} (e_{z_k|k} - \gamma e_{z_{k-1}|k-1})^T \right] \\ & [\text{Diag} (e_{z_{k+1}|k})]^{-1} S_{k+1} [\text{Diag} (e_{z_{k+1}|k})]^{-1} \\ & [\text{Diag} (e_{z_{k+1}|k} - \gamma e_{z_k|k})^T \\ & - \text{Diag} (e_{z_k|k} - \gamma e_{z_{k-1}|k-1})^T \mathbf{\Lambda}_{k+1}] \widehat{\mathbf{H}}^T \end{aligned} \quad (47)$$

Note that $\text{Diag}(e_z)$ transforms the measurement error vector into a diagonal matrix. The partial derivative in (40) is calculated as a summation of the partial derivative of the four parts presented by (44)–(47). These derivatives are calculated as:

$$\frac{\partial [\text{trace}(\text{Part 1})]}{\partial \mathbf{\Lambda}_{k+1}} = 0, \quad (48)$$

$$\begin{aligned} \frac{\partial [\text{trace}(\text{Part 2})]}{\partial \mathbf{\Lambda}_{k+1}} &= \widehat{\mathbf{H}}^{-T} \mathbf{P}_{k+1|k} \widehat{\mathbf{H}}^T \left[\text{Diag} (e_{z_{k+1}|k}) \right]^{-1} \\ & \text{Diag} (e_{z_k|k} - \gamma e_{z_{k-1}|k-1})^T \end{aligned} \quad (49)$$

$$\begin{aligned} \frac{\partial [\text{trace}(\text{Part 3})]}{\partial \mathbf{\Lambda}_{k+1}} &= \widehat{\mathbf{H}}^{-T} \mathbf{P}_{k+1|k} \widehat{\mathbf{H}}^T \left[\text{Diag} (e_{z_{k+1}|k}) \right]^{-1} \\ & \text{Diag} (e_{z_k|k} - \gamma e_{z_{k-1}|k-1})^T \end{aligned} \quad (50)$$

$$\begin{aligned} \frac{\partial [\text{trace}(\text{Part 4})]}{\partial \mathbf{\Lambda}_{k+1}} &= 2\widehat{\mathbf{H}}^{-1} \begin{bmatrix} \mathbf{\Lambda}_{k+1} \text{Diag} (e_{z_k|k} - \gamma e_{z_{k-1}|k-1}) \\ S_{k+1}^T [\text{Diag} (e_{z_{k+1}|k})]^{-1} \\ \text{Diag} (e_{z_k|k} - \gamma e_{z_{k-1}|k-1})^T \\ -\text{Diag} (e_{z_{k+1}|k} - \gamma e_{z_k|k})^T S_{k+1} \\ [\text{Diag} (e_{z_{k+1}|k})]^{-1} \\ \text{Diag} (e_{z_k|k} - \gamma e_{z_{k-1}|k-1})^T \end{bmatrix} \end{aligned} \quad (51)$$

where $\mathbf{S} \in \mathbb{R}^{m \times m}$ is a symmetric matrix, called the innovation covariance matrix (similar to the Kalman filter), and given by:

$$\mathbf{S}_{k+1} = \widehat{\mathbf{H}} \mathbf{P}_{k+1|k} \widehat{\mathbf{H}}^T + \mathbf{R}_k \quad (52)$$

Adding (48)–(51) and rearranging the resulting terms, the partial derivative of \mathbf{P} is obtained as:

$$\begin{aligned} & \mathbf{P}_{k+1|k} \widehat{\mathbf{H}}^T - \widehat{\mathbf{H}}^{-1} [\text{Diag}(e_{z_{k+1}|k} - \gamma e_{z_k|k})] \mathbf{S}_{k+1} \\ & = -\widehat{\mathbf{H}}^{-1} \mathbf{\Lambda}_{k+1} [\text{Diag}(e_{z_{k+1}|k})]^{-1} \\ & \text{Diag}[(e_{z_k|k} - \gamma e_{z_{k-1}|k-1})] \mathbf{S}_{k+1} = 0 \end{aligned} \quad (53)$$

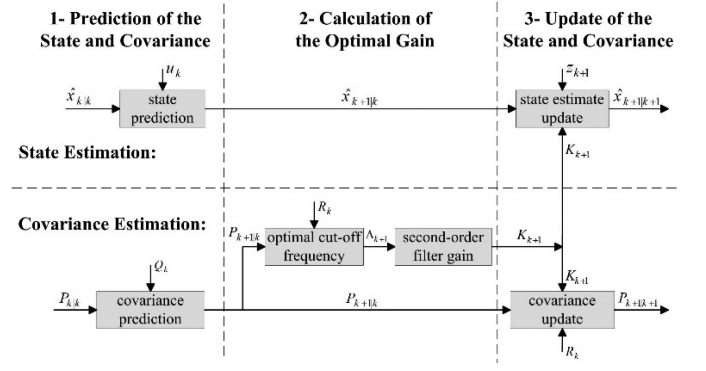


Figure 2. The optimal second-order filter for state estimation.

Solving equality (53) in terms of $\mathbf{\Lambda}$ results in the optimal cut-off frequency matrix as: $\mathbf{\Lambda}_{k+1} = [\text{Diag}(e_{z_{k+1}|k} - \gamma e_{z_k|k}) \mathbf{S}_{k+1} - \widehat{\mathbf{H}} \mathbf{P}_{k+1|k} \widehat{\mathbf{H}}^T]^{-1} [\text{Diag}(e_{z_k|k} - \gamma e_{z_{k-1}|k-1}) \mathbf{S}_{k+1}]^{-1}$ that is equal to (39). \square

The optimal second-order filter is summarised as follows:

1. Prediction Step:

- Prediction of the *a priori* state vector, measurement vector, and state error covariance matrix are, respectively, calculated as follows:

$$\begin{aligned} \widehat{\mathbf{x}}_{k+1|k} &= \widehat{\mathbf{F}} \widehat{\mathbf{x}}_{k|k} + \widehat{\mathbf{G}} \mathbf{u}_k \\ \widehat{\mathbf{z}}_{k+1|k} &= \widehat{\mathbf{H}} \widehat{\mathbf{x}}_{k+1|k} \\ \mathbf{P}_{k+1|k} &= \widehat{\mathbf{F}} \mathbf{P}_{k|k} \widehat{\mathbf{F}}^T + \mathbf{Q}_k \end{aligned} \quad (54)$$

2. Update Step:

- The innovation covariance matrix, cut-off frequency matrix, and corrective gain are, respectively, found by:

$$\begin{aligned} \mathbf{S}_{k+1} &= \mathbf{S}_{k+1} = \widehat{\mathbf{H}} \mathbf{P}_{k+1|k} \widehat{\mathbf{H}}^T + \mathbf{R}_k \\ \mathbf{\Lambda}_{k+1} &= [\text{Diag} (e_{z_{k+1}|k} - \gamma e_{z_k|k}) \mathbf{S}_{k+1} - \widehat{\mathbf{H}} \mathbf{P}_{k+1|k} \widehat{\mathbf{H}}^T] \\ & [\text{Diag} (e_{z_k|k} - \gamma e_{z_{k-1}|k-1}) \mathbf{S}_{k+1}]^{-1} \text{Diag} (e_{z_{k+1}|k}) \\ \mathbf{K}_{k+1} &= \widehat{\mathbf{H}}^{-1} [\text{Diag} [e_{z_{k+1}|k} - (\gamma + \mathbf{\Lambda}_{k+1}) e_{z_k|k}] \\ & + \gamma \mathbf{\Lambda}_{k+1} \text{Diag} (e_{z_{k-1}|k-1})] [\text{Diag} (e_{z_{k+1}|k})]^{-1} \end{aligned} \quad (55)$$

- Update of the *a priori* state vector and state error covariance matrix into the *a posteriori* estimates is calculated as:

$$\begin{aligned} \widehat{\mathbf{x}}_{k+1|k+1} &= \widehat{\mathbf{x}}_{k+1|k} + \mathbf{K}_{k+1} e_{z_{k+1}|k} \\ \mathbf{P}_{k+1|k+1} &= (\mathbf{I} - \mathbf{K}_{k+1} \widehat{\mathbf{H}}) \mathbf{P}_{k+1|k} (\mathbf{I} - \mathbf{K}_{k+1} \widehat{\mathbf{H}})^T \\ & + \mathbf{K}_{k+1} \mathbf{R}_{k+1} \mathbf{K}_{k+1}^T \end{aligned} \quad (56)$$

Figure 2 presents a block diagram of the optimal second-order filter for state estimation.

It is interesting to note that the corrective gain of the optimal second-order filter with the cut-off frequency

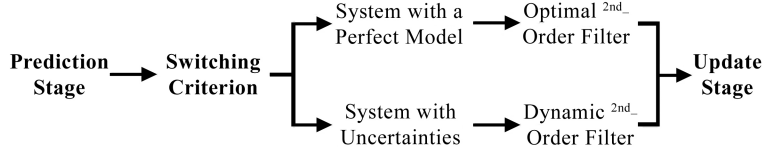


Figure 3. Main concept of the combined strategy for state estimation.

coefficient of (39) represents the Kalman filter gain in the absence of modelling uncertainties. In order to prove this equivalency, substitute the cut-off frequency coefficient (39) into the corrective gain (12) such that:

$$\mathbf{K}_{k+1} = \widehat{\mathbf{H}}^{-1} \begin{Bmatrix} \text{Diag} (e_{z_{k+1|k}} - \gamma e_{z_{k|k}}) - \\ \left[\text{Diag} (e_{z_{k+1|k}} - \gamma e_{z_{k|k}}) \mathbf{S}_{k+1} - \widehat{\mathbf{H}} \mathbf{P}_{k+1|k} \widehat{\mathbf{H}}^T \right] \\ \left[\text{Diag} (e_{z_{k|k}} - \gamma e_{z_{k-1|k-1}}) \mathbf{S}_{k+1} \right]^{-1} \\ \text{Diag} (e_{z_{k|k}} - \gamma e_{z_{k-1|k-1}}) \\ \text{Diag} (e_{z_{k+1|k}}) \left[\text{Diag} (e_{z_{k+1|k}}) \right]^{-1} \end{Bmatrix} \quad (57)$$

Rearranging (57), it becomes:

$$\mathbf{K}_{k+1} = \widehat{\mathbf{H}}^{-1} \begin{Bmatrix} \text{Diag} (e_{z_{k+1|k}} - \gamma e_{z_{k|k}}) - \\ \left[\text{Diag} (e_{z_{k+1|k}} - \gamma e_{z_{k|k}}) \mathbf{S}_{k+1} - \widehat{\mathbf{H}} \mathbf{P}_{k+1|k} \widehat{\mathbf{H}}^T \right] \\ \mathbf{S}_{k+1}^{-1} \left[\text{Diag} (e_{z_{k|k}} - \gamma e_{z_{k-1|k-1}}) \right]^{-1} \\ \text{Diag} (e_{z_{k|k}} - \gamma e_{z_{k-1|k-1}}) \end{Bmatrix} \quad (58)$$

where equality (58) may be restated as follows:

$$\mathbf{K}_{k+1} = \widehat{\mathbf{H}}^{-1} \left[\text{Diag} (e_{z_{k+1|k}} - \gamma e_{z_{k|k}}) - \text{Diag} (e_{z_{k+1|k}} - \gamma e_{z_{k|k}}) + \widehat{\mathbf{H}} \mathbf{P}_{k+1|k} \widehat{\mathbf{H}}^T \mathbf{S}_{k+1}^{-1} \right] \quad (59)$$

Simplifying equality (59), the corrective gain of the optimal second-order filter becomes:

$$\mathbf{K}_{k+1} = \mathbf{P}_{k+1|k} \widehat{\mathbf{H}}^T \mathbf{S}_{k+1}^{-1} \quad (60)$$

which is equal to the Kalman gain.

As presented in (60), the corrective gain of the optimal second-order filter collapses to the Kalman filter's gain and hence, its robustness is partially lost. In order to overcome this issue and preserve stability as well as optimality, a combined strategy is proposed similar to Gadsden's combined strategy introduced in [14], [17]. In this strategy, the dynamic second-order filter with the corrective gain (12) applies to systems with modelling uncertainties (*e.g.*, systems under fault conditions). The optimal second-order filter with the gain of (55) applies to systems with a known model (*e.g.*, systems under normal conditions). The combined strategy automatically switches between these two filters in order to preserve optimality for systems with a known model and at the same time preserves the stability for systems with uncertainties. Figure 3

presents a flow diagram of the combined strategy. The decision on the level of modelling uncertainties is made by comparing the statistical properties of the measurement error with the ones obtained for the system in the normal condition. In this context, there is a number of statistical tests that may be applied to the measurement error in order to evaluate modelling uncertainties. The easiest test for evaluating the level of uncertainties is to set a constant (or adaptive) threshold for the measurement error. If the error's mean value exceeds this threshold, the dynamic second-order filter is applied for state estimation. Meanwhile, there are more accurate tests performed on the probability distribution of the measurement error. Hwang *et al.* [25] summarised a number of these tests, including sequential probability ratio test, cumulative sum algorithm, and generalised likelihood ratio test.

5. The Dynamic Second-Order Filter for Systems with Fewer Measurements than States ($m < n$)

The dynamic second-order filter method may be applied to systems with fewer measurements than states $m < n$. The process of calculating the gain for hidden states is similar to what was presented for the SVSF method in [12]. In this context, the corrective gain relating to hidden states is derived using the Luenberger's observer [12]. Following *Assumption 2*, the linear system with (1) and (2) is completely observable. The state vector is decomposed into two parts $\mathbf{x} = [\mathbf{x}_u \ \mathbf{x}_l]^T$, where the upper part $\mathbf{x}_u \in \mathbb{R}^{m \times 1}$ is directly measured and the lower part $\mathbf{x}_l \in \mathbb{R}^{(n-m) \times 1}$ is not. Using the Luenberger's transformation, a new measurement vector is obtained by [12]:

$$\mathbf{T} \mathbf{x}_k = [\mathbf{y}_{u_k} \ \mathbf{y}_{l_k}]^T \quad (61)$$

where \mathbf{T} is a transformation matrix. In this regard, a revised state vector is formulated in terms of measurements such that: $\mathbf{y} = [\mathbf{z} \ \mathbf{y}_l]^T$, where $\mathbf{z} \in \mathbb{R}^{m \times 1}$ denotes the direct measurement vector and $\mathbf{y}_l \in \mathbb{R}^{(n-m) \times 1}$ denotes an artificial measurement vector. The problem is to calculate values for entries of \mathbf{y}_l based on the partitioned model. The measurement model is [12]:

$$\begin{bmatrix} \mathbf{z}_{k+1} \\ \mathbf{y}_{l_{k+1}} \end{bmatrix} = \begin{bmatrix} \Phi_{11} & \Phi_{12} \\ \Phi_{21} & \Phi_{22} \end{bmatrix} \begin{bmatrix} \mathbf{z}_k \\ \mathbf{y}_{l_k} \end{bmatrix} + \begin{bmatrix} \mathbf{G}_1 \\ \mathbf{G}_2 \end{bmatrix} \mathbf{u}_k + \mathbf{w}_k \quad (62)$$

where $\Phi = T^{-1}AT$, and $G = T^{-1}B$. The *a priori* state estimate is given by [12]:

$$\begin{bmatrix} \hat{z}_{k+1|k} \\ \hat{y}_{l_{k+1|k}} \end{bmatrix} = \begin{bmatrix} \hat{\Phi}_{11} & \hat{\Phi}_{12} \\ \hat{\Phi}_{21} & \hat{\Phi}_{22} \end{bmatrix} \begin{bmatrix} z_k \\ \hat{y}_{l_{k|k}} \end{bmatrix} + \begin{bmatrix} \hat{G}_1 \\ \hat{G}_2 \end{bmatrix} u_k \quad (63)$$

Subtracting (63) from (62), the *a priori* and *a posteriori* measurement error vectors for the projected measurement vector y_l are calculated as:

$$e_{y_{l_{k+1|k+1}}} = \hat{\Phi}_{12}^{-1} e_{z_{k+1|k}} \quad (64)$$

$$e_{y_{l_{k+1|k}}} = \hat{\Phi}_{22} \hat{\Phi}_{12}^{-1} e_{z_{k+1|k}} \quad (65)$$

where $e_{y_l} \in \mathbb{R}^{(n-m) \times 1}$ is the projected measurement error vector and $e_z \in \mathbb{R}^{m \times 1}$ is the measurement error vector corresponding to measurable states. (64) and (65) represent a mapping of the measurement error for calculating the filter gain. Further to (12), the corrective gain of the dynamic second-order filter for the lower partition of states is derived by substituting values of $e_{y_{l_{k|k}}}$ and $e_{y_{l_{k+1|k}}}$ into (12) as:

$$K_{k+1} = \left[\hat{\Phi}_{22} \hat{\Phi}_{12}^{-1} e_{z_{k+1|k}} - (\gamma + \Lambda) \hat{\Phi}_{12}^{-1} e_{z_{k|k-1}} + \gamma \Lambda \hat{\Phi}_{12}^{-1} e_{z_{k-1|k-2}} \right] \left[\hat{\Phi}_{22} \hat{\Phi}_{12}^{-1} e_{z_{k+1|k}} \right]^+ \quad (66)$$

By combining the gains of each partition, the filter gain is obtained for systems with fewer measurements than states as:

$$K_{k+1} = \begin{bmatrix} \hat{H}^+ [e_{z_{k+1|k}} - (\gamma + \Lambda) e_{z_{k|k}} + \gamma \Lambda e_{z_{k-1|k-1}}] \\ [e_{z_{k+1|k}}]^+ \\ \left[\hat{\Phi}_{22} \hat{\Phi}_{12}^{-1} e_{z_{k+1|k}} + \hat{\Phi}_{12}^{-1} [-(\gamma + \Lambda) e_{z_{k|k-1}} + \gamma \Lambda^{-1} e_{z_{k-1|k-2}}] \right] \left[\hat{\Phi}_{22} \hat{\Phi}_{12}^{-1} e_{z_{k+1|k}} \right]^+ \end{bmatrix} \quad (67)$$

Lemma 2: *The dynamic second-order filter under the corrective gain (66) is stable for the lower partition of states y_l .*

Proof: Consider a positive-definite Lyapunov function as follows:

$$V_k = (\Delta e_{j,y_{l,k|k}} + c_{jj} e_{j,y_{l,k|k}})^2, \quad j = 1, \dots, n-m \quad (68)$$

where $c_{jj} \in \mathbb{R}^{(n-m) \times (n-m)}$ is an element of the cut-off frequency matrix for the lower state partition, and e_{j,y_l} is an element of the measurement error vector for the lower partition state $e_{y_l} \in \mathbb{R}^{(n-m) \times 1}$. Steps (14) through (22) may simply be repeated for the above Lyapunov function. Following (64) and (65), as $e_{y_{l_{k+1|k+1}}} = \hat{\Phi}_{12}^{-1} e_{z_{k+1|k}}$, and $e_{y_{l_{k+1|k}}} = \hat{\Phi}_{22} \hat{\Phi}_{12}^{-1} e_{z_{k+1|k}}$, the corrective gain $K_{j,l}$ for the lower partition states is restated as:

$$K_{j,l_{k+1}} = \begin{bmatrix} e_{j,y_{l_{k+1|k}}} - (\gamma_{jj} + \lambda_{jj}) e_{j,y_{l_{k|k}}} + \gamma_{jj} \lambda_{jj} e_{j,y_{l_{k-1|k-1}}} \\ [e_{j,y_{l_{k+1|k}}}]^+ \end{bmatrix} \quad (69)$$

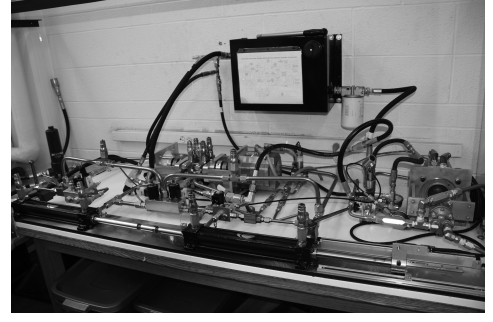


Figure 4. The EHA setup.

Using the above relation for the corrective gain and following steps (14) through (22) of the previous proof of stability, the time difference of the Lyapunov function (68) is obtained as:

$$\Delta V_{k+1} = (\gamma_{jj}^2 - 1) [(1 + \lambda_{jj}) e_{j,y_{l_{k|k}}} - e_{j,y_{l_{k-1|k-1}}}]^2 \quad (70)$$

As the convergence rate matrix $\gamma = \text{Diag}(\gamma_{jj}) \in \mathbb{R}^{(n-m)(n-m)}$ is defined such that $0 < \gamma_{jj} < 1$, it leads to $\Delta V_{k+1} < 0$ which proves the stability of the dynamic second-order filter under the gain (66) defined for the lower partition states. \square

6. Experiments Using an Aerospace Electro-Hydrostatic Actuator

In order to study the performance of the combined filtering strategy (dynamic second-order filter for uncertain systems and optimal version for normal systems) for state estimation, it is applied to an experimental EHA setup. The EHA setup has been designed and built in the Center for Mechatronics and Hybrid Technology at McMaster University [26]. Figure 4 presents the EHA experimental setup. Figure 5 shows the circuit diagram of the EHA setup with numbered elements. The EHA system is used to compare the performance of the combined strategy to other estimation methods, including the robust Kalman filter and the SVSF. The test is composed of three scenarios, including the normal EHA with a known model that contains noise and two faulty scenarios with unknown models that include the EHA with friction or internal leakage.

The EHA system shown in Fig. 5 uses pumping action (10) to create pressure and move piston A (3) and piston B (4). The EHA is composed of several components, including a symmetric linear actuator (8); a variable-speed electric motor (13); a bi-directional gear pump (10); a pressure relief valve (7); an accumulator (2); connecting tubes; and an inner circuit to prevent cavitation as shown in Fig. 5 by the dotted red line. The EHA setup includes complementary circuits that allow physical simulation of friction and leakage faults as shown in Fig. 5 by dotted black lines [17]. The hydraulic circuit of the EHA setup consists of two main parts. The first part is the inner low-pressure circuit that filters the oil. It uses an accumulator (2) and filters and checks valves (6) to keep the minimum system pressure at 40 *psi*. The inner circuit

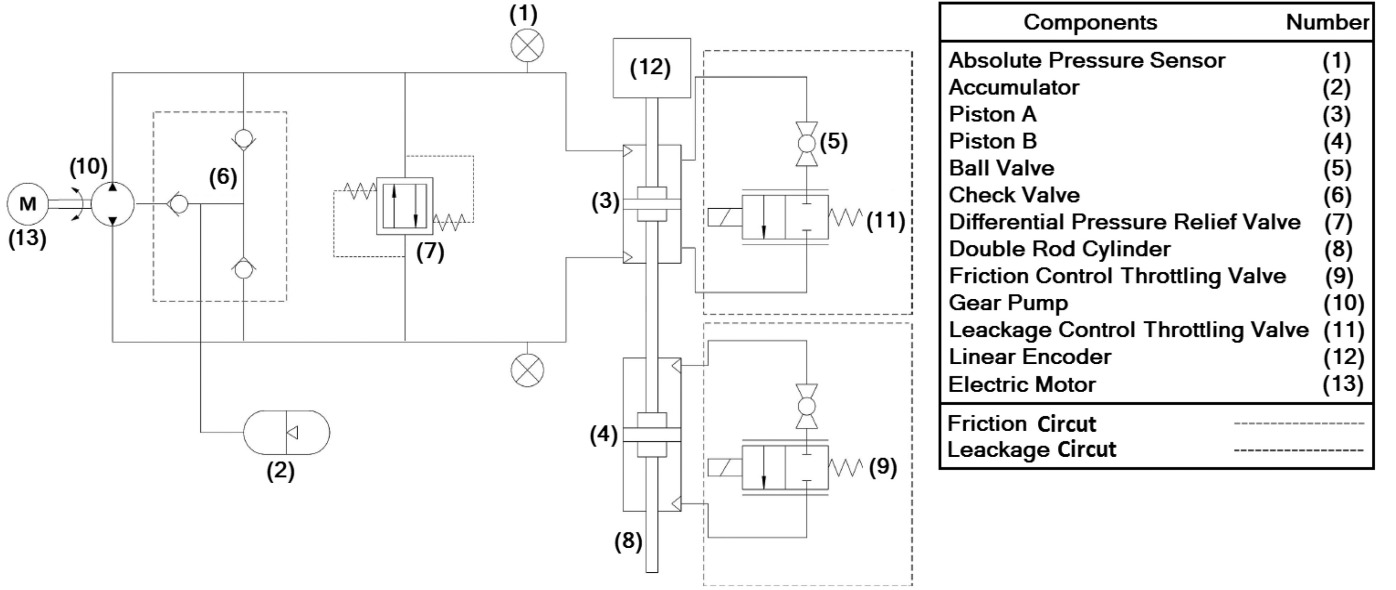


Figure 5. The circuit diagram of the EHA experimental setup (Upgraded from [17]).

prevents cavitation and circulates oil for compensating leakage. The second part of the hydraulic circuit is the outer high-pressure circuit that produces actuation. The variable-speed electric servomotor, which is a SIEMENS 1FK7080-5AF71-1AG2, drives the bi-directional gear pump (10) and circulates oil into cylinder (8). This causes a pressure differential across the actuating cylinder and results in the motion of the load. The speed of the gear pump (10) regulates the actuation performance by changing the oil flow rate. An accumulator (2) is used to prevent cavitation and to collect the case drain leakage from the gear pump (10). The pressure relief valve (7) is used to limit the maximum system pressure to 500 psi during experiments. The EHA's input is the voltage to the electric motor (13) that regulates the direction and the speed of the pump (10). The input voltage adjusts the value of the flow rate that in turn results in controlling the piston's position, velocity, and acceleration [17].

An optical linear encoder (12) attached to piston A is used to obtain position measurements. Two types of fault conditions may be physically induced, including internal leakage and friction. To simulate a friction fault condition in the EHA setup, piston A is used as the driving mechanism while piston B acts as a load. By changing the orifice size of the friction control throttling valve (9), the load may be varied allowing the physical simulation of friction faults. The orifice opening determines the level of severity of the fault condition. Similarly, internal leakage fault conditions can be physically simulated by using the leakage control throttling valve (5). Opening throttling valve (5) simulates cross-port leakage between the two chambers of cylinder (A). These simulated fault conditions change dynamics of the EHA system and inject modelling uncertainties in its state model.

The EHA dynamics may be described by using three state variables that are the actuator position $x_1 = x$, velocity $x_2 = \dot{x}$, and acceleration $x_3 = \ddot{x}$. A nonlinear

state-space model of the EHA is given by [17]:

$$x_{1,k+1} = x_{1,k} + T x_{2,k} \quad (71)$$

$$x_{2,k+1} = x_{2,k} + T x_{3,k} \quad (72)$$

$$x_{3,k+1} = \left[1 - T \frac{a_2 V_0 + M \beta_e L}{M V_0} \right] x_{3,k} - T \frac{(A_E^2 + a_2 L) \beta_e}{M V_0} x_{2,k} + T \frac{A_E \beta_e}{M V_0} - T \frac{a_1 V_0 x_{2,k} x_{3,k} + \beta_e L (a_2 x_{2,k}^2 + a_3)}{M V_0} \text{sgn}(x_{2,k}) \quad (73)$$

where A_E is the piston cross-sectional area, β_e is the effective bulk modulus, L is the leakage coefficient, M is the load mass, and V_0 is the initial cylinder volume. T denotes the sample time and is set at $T = 1$ ms. Table 1 presents the numerical values of these parameters. The input to the EHA system relates to flow and in a simplified form is given by [17]:

$$u = D_p \omega_p - \text{sgn}(-P_2) Q_{L0} \quad (74)$$

where D_p is the pump displacement, Q_l is the leakage flow rate, and Q_{l0} is the parameter used to adjust offsets. $\Delta P = P_1 - P_2$ is the differential pressure and is measured by a pressure sensor. A detailed procedure for physical modelling, linearisation, and parameter identification of the EHA is presented in [17].

In order to compare the performance of the dynamic second-order filter with the SVSF and the robust Kalman filter, the EHA normal model is used in the filters for state estimation under all conditions including the normal and faulty conditions. The duration of the experiment is 11 s. It starts with the EHA under the normal condition for the first three seconds, followed by the EHA under friction for the next four seconds, and ends with the EHA under leakage for the last four seconds. Figure 6 presents profiles of the input voltage and the measured actuator position under these three normal and faulty scenarios.

Table 1
Numeric Values of the EHA Parameters [17]

Parameter	Physical Meaning	Parameter Values
a_1	Friction coefficients	6.589×10^4
a_2		2.144×10^3
a_3		436
A_E	Piston area	$1.52 \times 10^{-3} \text{ m}^2$
D_p	Pump displacement	$5.57 \times 10^{-7} \text{ m}^3/\text{rad}$
L	Leakage coefficient	$4.78 \times 10^{-12} \text{ m}^3/(\text{sec} \times \text{Pa})$
M	Load mass	7.376 kg
Q_{L0}	Flow rate offset	$2.41 \times 10^{-6} \text{ m}^3/\text{sec}$
V_0	Initial cylinder volume	$1.08 \times 10^{-3} \text{ m}^3$
β_e	Effective bulk modulus	$2.07 \times 10^8 \text{ Pa}$

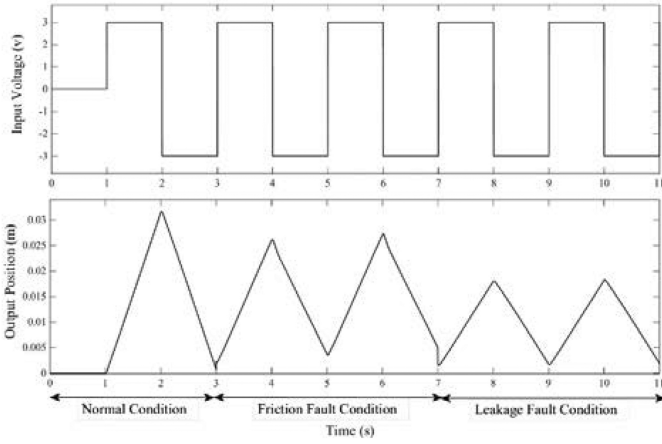


Figure 6. Profiles of the input voltage and output position under three scenarios.

Initial values of states are assumed zero and the sample time for discretisation is set to $T = 1 \text{ ms}$. The nonlinear model of the EHA, described by (71) through (74), may simply be linearised by calculating its partial derivatives at its equilibrium point: $\mathbf{x}(0) = [0 \ 0 \ 0]^T$. The linearised EHA model is hence given by:

$$\mathbf{x}_{k+1} = \mathbf{A}\mathbf{x}_k + \mathbf{B}u_k \quad (75)$$

where,

$$\mathbf{A} = \begin{bmatrix} 1 & T & 0 \\ 0 & 1 & T \\ 0 & -60.303 & 0.708 \end{bmatrix}, \quad \mathbf{B} = \begin{bmatrix} 0 \\ 0 \\ 39497 \end{bmatrix} \quad (76)$$

Accuracy and smoothness of state estimates provided by the combined strategy (dynamic/optimal second-order filter) are compared with those obtained by the robust Kalman filter and the SVSF methods. Note that the EHA model is third order, and position is the only

measured state. In order to estimate other states, the SVSF and the dynamic/optimal second-order filter need to use the strategy outlined in Section 5. All the inputs and initial conditions are the same for the three estimators. The initial state estimates $\hat{\mathbf{x}}_{0|0}$ and error covariance matrix $\mathbf{P}_{0|0}$ for the robust Kalman filter and the optimal second-order filter are the same and are equal to $\hat{\mathbf{x}}_{0|0} = [0 \ 0 \ 0]^T$, $\mathbf{P}_{0|0} = 10 \times \text{eye}(3)$. The convergence rate factors for the SVSF, and the combined strategy are set to $\gamma = 0.5$ and $\gamma = 0.1$, respectively. The cut-off frequency matrix for the dynamic second-order filter is set to: $\Lambda = 0.2 \times \text{eye}(3)$. For the SVSF, the smoothing boundary layer is set to $\varphi = [10^{-11} \ 10^{-7} \ 10^{-4}]^T$. The measurement noise covariance matrix \mathbf{R} for the robust Kalman filter, and the optimal second-order filter is equal to $\mathbf{R} = [10^{-13}]$. The process noise covariance matrix \mathbf{Q} for these methods is moreover equal to:

$$\mathbf{Q}_{\text{robust KF}} = \mathbf{Q}_{\text{optimal 2nd-filter}} = \begin{bmatrix} 10^3 & 0 & 0 \\ 0 & 10 & 0 \\ 0 & 0 & 10^2 \end{bmatrix} \quad (77)$$

The combined strategy automatically switches between the dynamic and the optimal second-order filters to make more accurate state estimates. In the EHA case, the switching index is defined as the squared value of the measurement error, as follows:

$$\Xi_k = e_{z_{k+1|k}}^2 \quad (78)$$

Based on the prior knowledge about the EHA, a threshold is defined for the position error measurements. In this test, the threshold is set to $0.3 \times 10^{-10} \text{ m}$. If the position measurement error is smaller than $0.3 \times 10^{-10} \text{ m}$, this means that the uncertainty level is small and, hence, the combined strategy selects the optimal second-order filter. Otherwise, if it is larger than the threshold, the uncertainty level is high, and the dynamic second-order filter is automatically

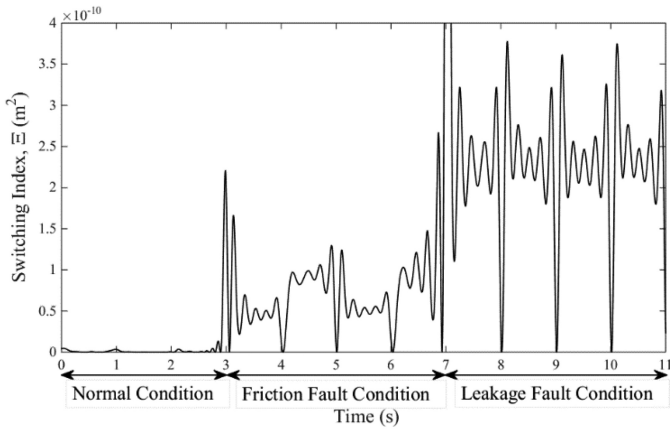


Figure 7. State estimate profiles for the EHA under the leakage fault condition.

selected. Figure 7 presents the switching index profile for the EHA under the described test scenario.

In order to compare state estimation methods, the root mean square (RMS), and standard deviation of the state estimation error $e_x = x - \hat{x}$ are used. For comparing state estimation results against actual values pertaining to the velocity x_2 and acceleration x_3 , these are obtained by taking the first and the second time derivatives of the position measurement signal, respectively. As differentiation results in added noise, a Butterworth filter is used to filter out the differentiation noise from the obtained velocity and acceleration signals. Tables 2 and 3 present the RMS and the STD indicators generated by the robust Kalman filter [5], SVSF [12], and the combined strategy.

As observed in Table 2, the RMS value of the error by the combined strategy is smaller than the ones obtained by the SVSF, and robust Kalman filters. This shows that the combined strategy (dynamic/optimal second-order filter) produces the most accurate estimates, followed by the SVSF and the robust Kalman filter. Under normal conditions, the combine strategy selects the optimal second-order filter with a gain that is optimal in terms of the mean-squared error. Moreover, for the EHA under friction or leakage fault conditions, the combined strategy selects the dynamic second-order filter that produces a robust corrective gain. This gain pushes the measurement error and its time difference to zero and this characteristic results in higher degrees of accuracy for state estimation. Following Table 3, the combined strategy produces the smallest STD, followed by the SVSF, and the robust Kalman filter. This confirms that the combined strategy can achieve smoother state estimates compared to other estimation methods. This is due to the second-order formulation of its corrective gain that provides further information for updating state estimates. Fig. 8 compares the state estimation profiles generated by the robust Kalman filter, and the combined strategy (optimal/dynamic second-order filter) with the actual state trajectories under the test scenario. Figure 8 presents that until $t = 3$ s (under normal conditions) the estimated state profiles follow the actual ones and thus the linearised EHA model precisely describes the EHA dynamics. Figure 9

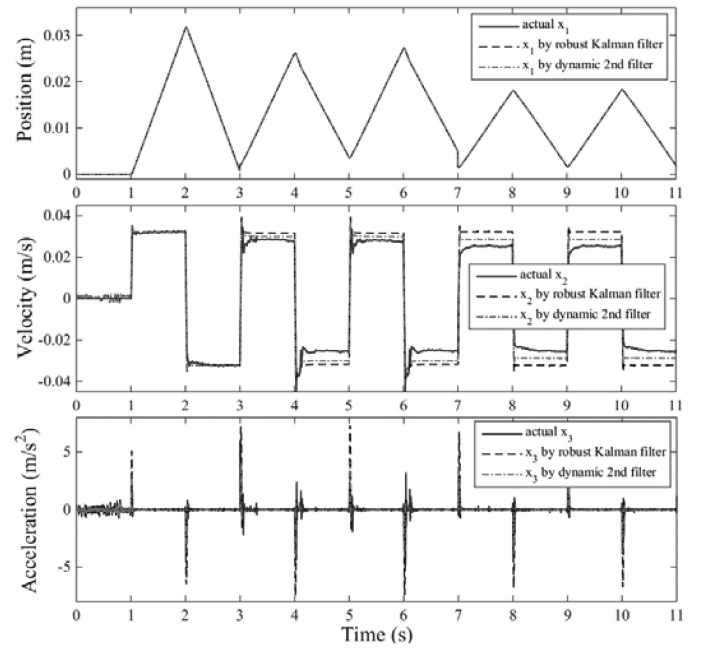


Figure 8. Profiles of the actual and the estimated states by different estimators.

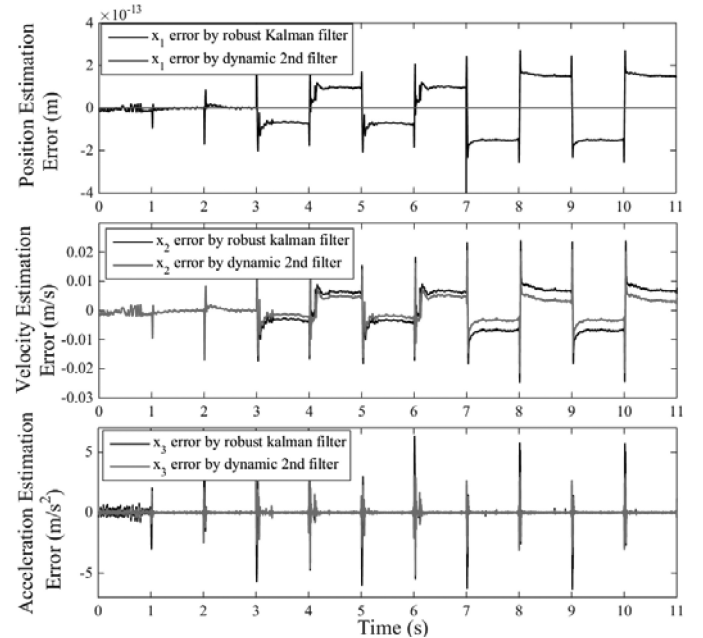


Figure 9. Profiles of the state estimation errors generated by different estimators.

presents profiles of the state estimation error generated by the robust Kalman filter and the combined strategy. Following Figs. 8 and 9, it is deduced that the combined strategy produces more accurate state estimates under fault conditions in which the EHA model contains huge but unknown modelling and parametric uncertainties.

Figure 10 presents the phase portraits of the measurement error (innovation sequence) and its time difference generated by the dynamic/optimal second-order filter for the EHA under normal and fault conditions. According to

Table 2
RMS Values of the State Estimation Error by Different Estimators

RMS	Robust Kalman Filter	SVSF	Dynamic/Optimal 2 nd -order Filter
Position (m)	3.35×10^{-19}	5.78×10^{-21}	1.24×10^{-23}
Velocity (m/s)	9.23×10^{-3}	7.55×10^{-3}	3.87×10^{-3}
Acceleration (m/s ²)	0.87	0.64	0.39

Table 3
Standard Deviations Values of the State Estimation Error by Estimators

STD	Robust Kalman Filter	SVSF	Dynamic/Optimal 2 nd -order Filter
Position (m)	4.11×10^{-19}	7.09×10^{-21}	1.23×10^{-23}
Velocity (m/s)	9.92×10^{-3}	7.81×10^{-2}	2.23×10^{-2}
Acceleration (m/s ²)	0.93	0.72	0.38

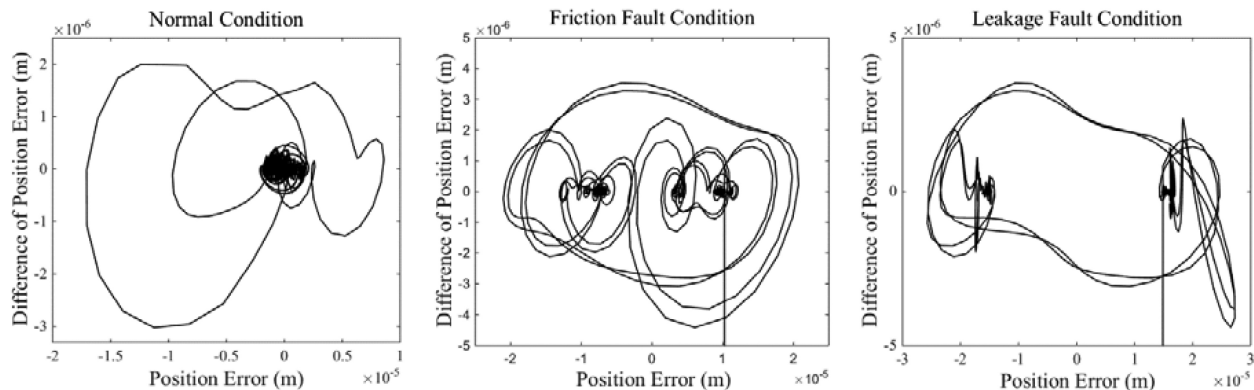


Figure 10. Phase portraits of the measurement error and its difference by the dynamic/optimal second-order filter under three scenarios.

these phase portraits, both the measurement error and its difference are decreasing over time below an upper bound (*e.g.*, ε_s). However, due to the measurement noise and uncertainties, the measurement error cannot be cancelled completely and remains norm-bounded. An advantage presented by the dynamic second-order filter is that it causes the measurement error and its difference to remain norm-bounded, even under uncertain faulty conditions. Note that following *Lemma 1* and equality (30), where $\Delta = 0.2$ and $\gamma = 0.1$, the state estimation error equation is obtained by: $[z^2 - 0.3z + 0.04]\bar{e}_x(z) = 0$. In this context, as the poles of this equation are within the unit circle, the state estimation error is stable given norm-bounded noise and uncertainties.

7. Conclusions

In this paper, the dynamic second-order filter is firstly introduced for state estimation of systems with linear state and measurement models. Its corrective gain is obtained using a linear manifold defined in terms of the measurement error (innovation sequence) and its time difference. The stability and convergence of this method is

then proven using the Lyapunov's second law of stability. The linear manifold introduces a cut-off frequency matrix into the filter formulation that filters out high-frequency dynamics. It operates like a first-order low-pass filter with an adjustable cut-off frequency that is related to the slope of the linear manifold. The gain of the dynamic second-order filter updates the *a priori* state estimates based on available information of the measurement error from the last two steps. This yields smoother state estimates with smaller dispersions over the robust Kalman filter.

In order to optimise the dynamic second-order filter, an optimal value of the cut-off frequency matrix is calculated such that the error's covariance matrix is minimised. It is shown that the gain of the optimal second-order filter is equivalent to the Kalman filter gain under ideal conditions at the expense of robustness. To achieve robustness and optimality, a combined strategy is presented that includes both the dynamic and optimal second-order filtering methods. The switching criterion is designed based on the statistical properties of the measurement error. The combined strategy automatically selects the optimal second-order filter for systems with a known model and the dynamic second-order filter for systems with modelling

uncertainties. The combined strategy is applied to an experimental EHA setup for estimation under normal and faulty conditions. Its performance is then compared with the robust Kalman filter and the SVSF methods. Experimental results confirm the main advantages of the combined strategy over the other two in terms of its greater accuracy and smoothness. Experiments moreover verify that the combined strategy pushes the measurement error and its difference towards zero. It was shown that they remain norm-bounded under normal and uncertain faulty conditions. Future research involves application of the proposed second-order filter for other systems with unknown uncertainties. They include maneuvering target tracking, battery management systems, and fault-tolerant control systems.

Data Sharing and Data Availability: Data sharing not applicable to this article as no datasets were generated or analysed during the current study.

References

- [1] M.S. Grewal and A.P. Andrews, *Kalman filtering: Theory and practice using MATLAB*, 2nd ed. (New York, NY: Wiley, 2001).
- [2] A.J. Krener, Kalman-Bucy and minimax filtering, *IEEE Transactions on Automatic Control*, 25(2), 1980, 291–292.
- [3] M. Milanese and R. Tempo, Optimal algorithms theory for robust estimation and prediction, *IEEE Transactions on Automatic Control*, 30(8), 1985, 730–738.
- [4] S. Zhuk, Minimax state estimation for linear discrete-time differential-algebraic equations, *Automatica*, 46(11), 2010, 1785–1789.
- [5] L. Xie, Y.C. Soh, and C.E. de Souza, Robust Kalman filtering for uncertain discrete-time systems, *IEEE Transactions on Automatic Control*, 39(6), 1994, 1310–1314.
- [6] T.H. Lee, W.S. Ra, T.S. Yoon, and J.B. Park, Robust Kalman filtering via krein space estimation, *IEE Proceedings of Control Theory and Applications*, 151(1), 2004, 59–63.
- [7] F. Wang and V. Balakrishnan, Robust Kalman filters for linear time-varying systems with stochastic parametric uncertainties, *IEEE Transactions on Signal Processing*, 50(4), 2002, 803–813.
- [8] A.H. Sayed, A framework for state-space estimation with uncertain models, *IEEE Transactions on Automatic Control*, 46(7), 2001, 998–1013.
- [9] D. Simon, *Optimal state estimation: Kalman, H-infinity, and nonlinear approaches*. (Hoboken, NJ: Wiley, 2006).
- [10] M. Fu, C.E. de Souza, and L. Xie, H_∞ estimation for uncertain systems, *International Journal of Robust and Nonlinear Control*, 2(2), 1992, 87–105.
- [11] B. Hassibi, A.H. Sayed, and T. Kailath, *Indefinite quadratic estimation and control: A unified approach to H_2 and H -infinity theories*. (Philadelphia, PA: SIAM Studies in Applied and Numerical Mathematics, 1999).
- [12] S.R. Habibi, The smooth variable structure filter, *Proceedings of the IEEE*, 95(5), 2007, 1026–1059.
- [13] S.R. Habibi and R. Burton, The variable structure filter, *ASME Journal of Dynamic Systems, Measurement and Control*, 125(3), 2003, 287–293.
- [14] S.A. Gadsden and S.R. Habibi, A new robust filtering strategy for linear systems, *Journal of Dynamic Systems, Measurement, and Control*, 135(1), 2013, 14503.
- [15] G. Zames, Feedback and optimal sensitivity: Model reference transformations, multiplicative seminorms, and approximate inverses, *IEEE Transactions on Automatic Control*, 26(2), 1981, 301–320.
- [16] D. Simon, From here to infinity, *Embedded Systems Programming*, 14(11), 2000, 20–32.
- [17] S.A. Gadsden, Y. Song, and S. Habibi, Novel model-based estimators for the purposes of fault detection and diagnosis, *IEEE/ASME Transactions on Mechatronics*, 18(4), 2013, 1237–1249.
- [18] A.K. Mahalanabis and M. Farooq, A second-order method for state estimation of non-linear dynamical systems, *International Journal of Control*, 14(4), 1971, 631–639.
- [19] A. Zanj and H. Afshari, Dynamic analysis of a complex pneumatic valve using pseudo-bondgraph simulation technique, *Journal of Dynamic Systems, Measurement, and Control*, 135(3), 2013, 34502.
- [20] H.H. Afshari, A. Zanj, and A.B. Novinzadeh, Dynamic analysis of a nonlinear pressure regulator using bondgraph simulation technique, *Journal of Simulation, Modeling, Practice and Theory*, 18(2), 2010, 240–252.
- [21] H.H. Afshari, S.A. Gadsden, and S.R. Habibi, Robust fault diagnosis of an electro-hydrostatic actuator using the novel dynamic second-order SVSF and IMM strategy, *International Journal of Fluid Power*, 15(3), 2014, 181–196.
- [22] H.H. Afshari, S. Gadsden, and S. Habibi, Condition monitoring of an electro-hydrostatic actuator using the dynamic 2nd-order smooth variable structure filter, *Proc. ASME Int. Design Engineering Technical Conf.*, Boston, MA, 2015, 1–6.
- [23] H.H. Afshari, D. Al-Ani, and S. Habibi, State estimation of a faulty actuator using the second-order smooth variable structure filter (the 2ND-order SVSF), *Proc. 28th IEEE Canadian Conf. Electrical and Computer Engineering*, Halifax, NS, 2015, 919–924.
- [24] M.S. Pedersen and K.B. Petersen, *The matrix cookbook*. (Copenhagen: Technical University of Denmark, 2008).
- [25] I. Hwang, S. Kim, Y. Kim, and C.E. Seah, A survey of fault detection, isolation, and reconfiguration methods, *IEEE Transactions on Control Systems Technology*, 18(3), 2010, 636–653.
- [26] S.A. Gadsden, *Smooth variable structure filtering: Theory and applications*, Ph.D. Thesis, McMaster University, Hamilton, ON, Canada, 2011.
- [27] M. Avzayesh, M. Abdel-Hafez, M. Al-Shabi, and S.A. Gadsden, The smooth variable structure filter: A comprehensive review, *Digital Signal Processing*, 110, 2021, 102912.
- [28] N.Y. Ko and T.G. Kim, Filtering method for location estimation of an underwater robot, *International Journal of Robotics and Automation*, 3(3), 2014, 168–183.

Biographies



Hamed H. Afshari earned the Ph.D. degree from McMaster University in the area of mechanical engineering. His research areas include estimation theory with application to mechatronic and aerospace systems. His current research interests include the area of data science and machine learning with application to aerospace systems.



Andrew S. Lee earned the Ph.D. degree from the University of Guelph in mechanical engineering. His specialisation is in the area of estimation theory, signal processing, and mechatronics. Before earning his doctorate, he obtained his Bachelor's degree of Mechanical Engineering from the University of Maryland, Baltimore County. He is currently a Research Engineer with Northrop Grumman in Maryland, USA.



S. Andrew Gadsden is an Associate Professor with the Department of Mechanical Engineering, McMaster University and is the Director of the Intelligent and Cognitive Engineering (ICE) Laboratory. His research area includes control and estimation theory, artificial intelligence and machine learning, and cognitive systems. He completed the Bachelor's degree in mechanical engineering and management

(business) and then earned the Ph.D. degree in mechanical engineering from McMaster University in the area of estimation theory with applications to mechatronics and aerospace systems. Before joining McMaster University, he was an Associate/Assistant Professor with the University of Guelph and an Assistant Professor with the Department of Mechanical Engineering, University of Maryland, Baltimore County, USA. He worked and continues to work with a number of colleagues in NASA, National Institute of Standards and Technology (NIST), U.S. Army Research Laboratory (ARL), and the US Department of Agriculture (USDA). He is an elected Fellow of ASME, is a Senior Member of IEEE, and is a Professional Engineer of Ontario. He is also a certified Project Management Professional (PMP).



Saeid R. Habibi is a Tier I Canada Research Chair, a Senior NSERC Industrial Research Chair, and a Full Professor with the Department of Mechanical Engineering, McMaster University. He joined McMaster in 2006, was promoted to the rank of Full Professor in 2008, and was the Chair of the Department of Mechanical Engineering from 2008 to 2013.

He obtained his Ph.D. degree in control engineering from the University of Cambridge, U.K., in 1990. His academic background includes research into artificial intelligence, intelligent control, state and parameter estimation, fault diagnosis and prediction, variable structure systems, actuation systems, mechatronics, and fluid power. The application areas for his research have included autonomous vehicles, traffic monitoring, automotive powertrain, aerospace, and robotics.